



# Modelling dispersal of sea scallop (*Placopecten magellanicus*) larvae on Georges Bank: The influence of depth-distribution, planktonic duration and spawning seasonality

C.S. Gilbert<sup>a,\*</sup>, W.C. Gentleman<sup>a</sup>, C.L. Johnson<sup>b</sup>, C. DiBacco<sup>b</sup>, J.M. Pringle<sup>c</sup>, C. Chen<sup>d</sup>

<sup>a</sup> Department of Engineering Mathematics and Internetworking, Dalhousie University, 1340 Barrington St., Halifax, NS, Canada B3J 1Y9

<sup>b</sup> Fisheries and Oceans Canada, Bedford Institute of Oceanography, Dartmouth, NS, Canada B2Y 4A2

<sup>c</sup> Department of Earth Sciences, and the Institute of Earth, Oceans & Space, University of New Hampshire, Durham, NH 03824, USA

<sup>d</sup> School of Marine Science and Technology, University of Massachusetts-Dartmouth, 706 South Rodney French Blvd., New Bedford, MA 02744, USA

## ARTICLE INFO

### Article history:

Available online 5 November 2010

## ABSTRACT

The giant sea scallop (*Placopecten magellanicus*) metapopulation on Georges Bank (GB) in the northwest Atlantic constitutes an economically important fishery, which is sustained by retention of planktonic larvae that are advected among three subpopulations. Dispersal of GB scallop larvae spawned in the fall is known to be sensitive to climate-related variability in the currents. Associated changes in temperature and stratification may elicit variations in biological responses that can also affect transport and these need to be examined. Additionally, no investigation has been made into transport of larvae spawned in spring, despite this being a consistently recurring phenomenon. Here, we quantified the influence of larval depth-distribution, planktonic larval duration (PLD) and spawning phenology on the retention and exchange of *P. magellanicus* larvae on GB. We developed a 3-D particle-tracking model to simulate larval transport in both spawning seasons using realistic circulation fields and assumptions about both larval behavior and PLD. Results were analyzed in terms of settlement distributions and dispersal matrices. Passive vertical behavior led to unrealistic depth-distribution in fall, while pycnocline-seeking behavior improved predicted settlement distributions and altered dispersal by factors of 2–5 for certain subpopulations. Simulations examining temperature-dependent larval development demonstrated significant effects of thermal history on PLD, and that associated changes in mean PLD of a few days can greatly alter connectivity. Larval transport in the spring exhibited increased downstream losses as well as sensitivity of retention to larval depth and spawning location. Our results demonstrate that biological factors significantly influence larval dispersal, and we need to reduce the uncertainty associated with estimates of these factors in order to predict effects of climate change on population connectivity.

© 2010 Elsevier Ltd. All rights reserved.

## 1. Introduction

Spatially separated populations of marine planktonic organisms can be advectively connected, and such connectivity plays a fundamental role in the dynamics of these subpopulations, as well as the metapopulation they form (Botsford et al., 2009; Cowen and Sponagule, 2009). Local retention and exchange among subpopulations results from complex interactions of the circulation with spawning phenology, duration of planktonic phase, and depth-selective behaviors (Hill, 1991; Hannah et al., 1998; Shanks, 2009; Fiksen et al., 2007). Because transport is influenced by environmental conditions, the ability to predict the effect of climate change requires a process-oriented understanding of larval dispersal. This was the motivation behind many GLOBEC studies in the northwest Atlantic on Georges Bank (GB), because this area is

both highly productive and highly sensitive to environmental variability (Butman and Beardsley, 1987; GLOBEC, 1992). GLOBEC GB targeted larval cod and haddock and their planktonic prey, but other economically and ecologically important species are endemic to GB, including the giant sea scallop *Placopecten magellanicus*, whose early life stages are planktonic (Hart and Chute, 2004; Naidu and Robert, 2006). Larval exchange among *P. magellanicus* subpopulations on GB is of particular importance as the upstream supply is negligible (Tremblay and Sinclair, 1992), and GB scallops constitute a self-sustaining metapopulation (Tremblay et al., 1994).

There are three major scallop aggregations on GB, which are typically considered as distinct subpopulations (Fig. 1; Tremblay et al., 1994; Hart and Chute, 2004). Transport of larvae among these subpopulations is principally driven by the tidal mixing front recirculation, along-shelf currents, and wind-induced variation in surface flows (Tremblay et al., 1994; Tian et al., 2009a). Previous studies indicate that the Great South Channel (GSC) subpopulation is the most retentive, receiving larvae spawned in both the

\* Corresponding author. Tel.: +1 902 494 6085.

E-mail address: [Chad.Gilbert@Dal.ca](mailto:Chad.Gilbert@Dal.ca) (C.S. Gilbert).

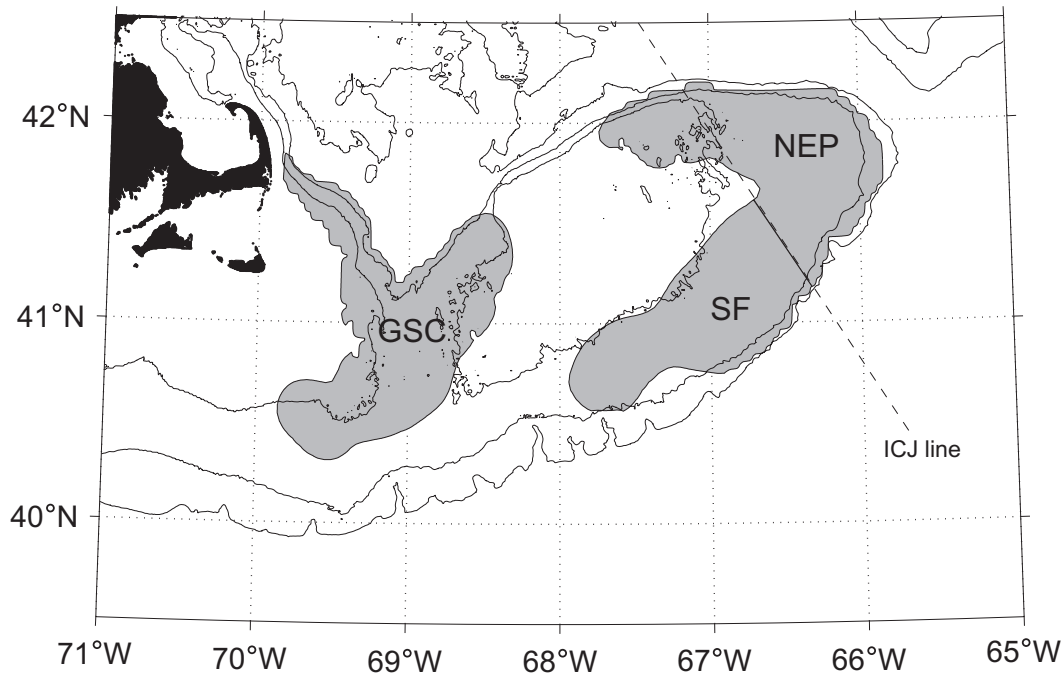


**Fig. 1.** The three scallop beds (subpopulations) – Great South Channel (GSC), Southern Flank (SF) and Northeast Peak (NEP) – on Georges Bank (GB). The International Court of Justice Line (labeled ICJ line) divides the Canadian and US exclusive economic zones. Also shown are the 60 m, 100 m and 200 m isobaths.

Northeast Peak (NEP) and Southern Flank (SF), as well as retaining locally spawned larvae (Tremblay et al., 1994). In contrast, local retention of larvae spawned in the NEP and SF subpopulations is negligible, and they rely mainly on input of larvae spawned in the GSC (Tremblay et al., 1994; Tian et al., 2009a). The GB meta-population also seeds downstream scallop beds along the New-England Shelf and Mid-Atlantic Bight (Tian et al., 2009a).

Exchange patterns of *P. magellanicus* larvae are dependent on environmental conditions, as variation in the winds and stratification affects GB circulation (Naimie et al., 1994, 2001; Pringle, 2006). Model estimates of larval retention on GB exhibited a 5-fold variation over eleven years, and the range in retention of GSC-spawned larvae was more than double that of the NEP or SF (Tian et al., 2009a). High frequency variation in the currents may also affect larval connectivity (Tian et al., 2009b). Moreover, variations in temperature and/or stratification may elicit different biological responses, and previous studies indicate that changes in swimming and growth can have significant effects on larval transport (e.g. Tremblay et al., 1994; Tian et al., 2009a).

Larval depth-distribution can influence dispersal because of vertical shear in the currents. Model sensitivity analyses that compared swimming behaviors (e.g. passive, fixed depth, surface-seeking) for *P. magellanicus* larvae demonstrated a significant effect on transport. Retention on GB was lower for shallower larvae, higher for larvae deeper in the water column, and bed connectivity varied by ~50% among the candidate behaviors (Tremblay et al., 1994; Tian et al., 2009a). More study of the influence of depth-distribution is needed because behaviors simulated in previous studies were simplified and may not have been sufficiently realistic (Tremblay et al., 1994). For example, no simulations have been made in which larvae maintain themselves near the pycnocline as would be consistent with observations (Tremblay and Sinclair, 1992).

For scallops, the planktonic larval duration (PLD) corresponds to the development time from hatch to settlement, which varies with temperature (Tremblay et al., 1994). The PLD of *P. magellanicus* on GB is typically assumed to be ~35 days in the fall based on mean

temperature (Tremblay et al., 1994), but changes in this value of PLD affect simulated larval drift. A shorter PLD reduces dispersal distances, increasing the connectivity from GSC to NEP, whereas a longer PLD is associated with increased loss of larvae from GB (Tremblay et al., 1994). Because temperatures on GB exhibit pronounced spatial and temporal variability (Naimie et al., 1994), PLDs likely vary among individuals due to differences in their thermal histories (Neuheimer and Taggart, 2007; Metaxas and Saunders, 2009). However, the effect this has on larval dispersal has not been investigated.

Another important factor for larval transport may be spawning seasonality. All previous modelling of *P. magellanicus* has been limited to larvae spawned in the fall, as that is the dominant spawning period (mid-September; Tremblay et al. 1994; Tian et al., 2009a). However, *P. magellanicus* is also consistently observed to spawn in the spring (May–June, DiBacco et al., 1995), and persistence of this spring spawn suggests it provides an adaptive advantage to the scallops. While circulation in the spring is generally in the same direction as in the fall, residual currents are slower and the around-bank gyre is weaker prior to the development of stratification (Naimie et al., 1994, 2001). Dispersal of larval scallops in the spring is likely dependent on depth-distributions and PLD, as these factors have been shown to be critical for other planktonic species on GB in this season (Werner et al., 1993; Miller et al., 1998; Lynch et al., 1998; Lough and Manning, 2001). The influence of the spring spawn on connectivity among GB subpopulations has yet to be assessed.

As a complement to recent studies on the role of interannual variability in the circulation (Tian et al., 2009a), we used a particle-tracking model to quantify the influence of biological factors on the dispersal of *P. magellanicus* larvae on GB. Specifically, we examined how interactions of climatological flows with variations in (1) depth-distribution, (2) temperature-dependent PLD, and (3) spawning seasonality affect larval transport. By assessing the extent to which these factors affect retention and exchange among GB subpopulations, this work improves our understanding of the governing processes, and helps direct future research programs

by identifying the kinds of data needed to predict the response of the GB scallop metapopulation to climate change.

## 2. Methods

### 2.1. Model description

We developed a 3D particle-tracking model to simulate drift of *P. magellanicus* larvae on GB. Transport of individual larvae (indexed by *ind*) was simulated from the time and geographic location of spawning (i.e.  $x_{ind}(t_{spawn,ind})$ ,  $y_{ind}(t_{spawn,ind})$ ) to the time and location of settlement (i.e.  $x_{ind}(t_{settle,ind})$ ,  $y_{ind}(t_{settle,ind})$ ). Spawning time was chosen to correspond with the temporal mid-point observed for each season (September 20th in the fall, May 16th in the spring; DiBacco et al., 1995 and unpublished data). We assumed that settlement time occurs at the end of the prescribed planktonic larval duration (PLD<sub>ind</sub>, described below). Horizontal transport was governed by horizontal advection, such that the change in position over a time step ( $\Delta t$ ) was computed as

$$\begin{aligned} x_{ind}(t + \Delta t) &= x_{ind}(t) + u_{adv}(x_{ind}, y_{ind}, z_{ind}, t) \Delta t \\ y_{ind}(t + \Delta t) &= y_{ind}(t) + v_{adv}(x_{ind}, y_{ind}, z_{ind}, t) \Delta t \end{aligned} \quad (1)$$

where  $u_{adv}$  and  $v_{adv}$  are the *x*- and *y*-components of the currents.

Vertical transport was based on assumptions about larval swimming, which changes with larval size and stage (Culliney, 1974; Chia et al., 1984; Tremblay et al., 1994). After hatching, the first swimming stage (trochophores) ascends at  $\sim 0.1$  mm/s over a period of 1–2 days at which time the veliger larval stage is reached. These larger pelagic larvae can swim upward at ranges of 0.1–1.3 mm/s. When ready to settle, they descend at rates  $\sim 1.7$  mm/s. Larvae may exhibit small vertical excursions from the bottom to search for appropriate benthic substrate prior to settling. We have chosen to neglect the ascent and descent, as the time scales associated with these are  $< 3$  days (Tremblay et al., 1994), over which period there would be only small horizontal displacements. The scallops may also occupy a bottom searching phase, but the characteristics are unknown, and so this behavior was also not simulated. Vertical transport was therefore simulated for two contrasting behavioral assumptions, hereafter referred to as *passive* and *pycnocline-seeking*. For *passive* behavior, swimming was considered negligible in comparison with vertical currents and turbulence. Thus, vertical transport was computed as

$$\begin{aligned} z_{ind}(t + \Delta t) &= z_{ind}(t) + w_{adv}(x_{ind}, y_{ind}, z_{ind}, t) \Delta t \\ &\quad + \Delta z_{turb}(x_{ind}, y_{ind}, z_{ind}, t) \end{aligned} \quad (2)$$

where  $w_{adv}$  is the vertical advective velocity, and  $\Delta z_{turb}$  is a random walk based on the local values of the turbulent mixing coefficient,  $k(x_{ind}, y_{ind}, z_{ind}, t)$ . The random walk was calculated using the standard Visser algorithm with a small time step,  $d\tau \ll \Delta t$ , in order to accurately simulate particle dispersion (Visser, 1997). Visser (1997) recommends use of a  $d\tau$  small enough to satisfy a criterion based on vertical variation in  $k$ . Choosing  $d\tau = 75$  s satisfied this criterion over most of our model domain, except for some shallow highly-mixed regions where the required time step was computationally prohibitive (i.e.  $d\tau \ll 1$  s). Hence, for particles in these select regions an alternative approach was used in which  $z_{ind}(t + \Delta t)$  was sampled from a uniform distribution of depths within the water column. This strategy resulted in modelled larval depth-distribution that is both consistent with Visser predictions as well as observations in such well-mixed regions (Tremblay and Sinclair, 1990). For the *pycnocline-seeking* behavioral assumption, vertical distributions were intended to reflect observations that *P. magellanicus* larvae are aggregated at the pycnocline in stratified regions (Tremblay and Sinclair, 1990). Hence, in *stratified* regions, modelled vertical transport was computed as:

$$z_{ind}(t + \Delta t) = z_{pycno}(x_{ind}, y_{ind}, z_{ind}, t + \Delta t), \quad (3)$$

and where the water was *well-mixed*, vertical transport was computed using Eq. (2).

Modelled PLD<sub>ind</sub> was based on assumptions about how long it takes larvae to grow to their size at settlement ( $\sim 240$ – $300$   $\mu\text{m}$ , Tremblay et al., 1994). At typical fall temperatures (i.e.  $12$ – $15$   $^{\circ}\text{C}$ ), growth rates are  $5$ – $6$   $\mu\text{m d}^{-1}$  and the corresponding larval development time is  $30$ – $40$  days (Tremblay et al., 1994). Here, temperature is assumed to affect growth with a  $Q_{10} = 2$ , as indicated for the related species *Pecten maximus* (Beaumont and Barnes, 1992). Thus, for an ambient temperature  $T_{ind} = T(x_{ind}, y_{ind}, z_{ind}, t)$ , the change in the individual's size ( $l_{ind}$ ) over the time step  $\Delta t$  was computed as

$$l_{ind}(t + \Delta t) = l_{ind}(t) + g_{ind}(T_{ind}) \Delta t \quad (4)$$

where the individual's growth rate  $g_{ind}(T) = g(13.5^{\circ}\text{C}) Q_{10}^{(T_{ind}-13.5)/10}$ . We defined  $g(13.5^{\circ}\text{C}) = 5.7$   $\mu\text{m d}^{-1}$ , and PLD<sub>ind</sub> as the time required to grow from  $l_{ind}(t_{spawn}) = 70$   $\mu\text{m}$ , to  $l_{ind}(t_{settle}) = 270$   $\mu\text{m}$ . These parameter values were chosen such that PLD<sub>ind</sub>( $13.5^{\circ}\text{C}$ ) =  $35.1$  d in order to facilitate comparison with fall simulations for which PLD =  $35$  d for all larvae.

### 2.2. Simulated environment

The physical environment (i.e. currents, turbulence, density, temperature) was characterized using output from the Finite-Volume Coastal Ocean Model (FVCOM) applied to the Gulf of Maine and forced with monthly mean hydrography and winds (Chen et al., 2003; Pringle, 2006). In order to reduce computational costs by use of a large advective time step ( $\Delta t = M2$  tidal period =  $12.42$  h), our particle-tracking model input Lagrangian residual quantities (i.e. the average quantity seen by a particle as it is displaced over one tidal cycle; Zimmerman, 1979). Temporal evolution of these fields was simulated by linear interpolation in time between months (see Johnson et al., 2006). The pycnocline depth,  $z_{pycno}(x, y, t)$  was estimated using a threshold definition (Thomson and Fine, 2003) applied to the local instantaneous density field ( $\rho(x, y, z, t)$ ). This threshold was chosen to be  $\Delta\rho = 0.6$   $\text{kg/m}^3$ , as it provides estimates of  $z_{pycno}$  that are consistent with observations for September (Tremblay and Sinclair, 1990; Tremblay et al., 1994). Locations where this threshold was not reached within the upper  $40$  m of the water column were considered *well-mixed*, whereas locations where the pycnocline was successfully identified by this algorithm were considered *stratified*.

Both spring and fall residual circulation demonstrate the classic GB features: (i) an anti-cyclonic gyre associated with the tidal mixing front roughly along the  $60$  m isobath and (ii) fast along-shelf currents on the outer flanks roughly between the  $60$  and  $200$  m isobaths (Naimie et al., 1994, 2001). Flow in the fall is somewhat faster ( $8.4$   $\text{cm/s}$  vs.  $6.7$   $\text{cm/s}$ ), due to seasonal variations in winds, temperatures and stratification. Surface temperatures decrease over the fall months (September–November), with the range varying among GB subregions (Fig. 2). The NEP is consistently the coldest subregion ( $\sim 15$ – $11$   $^{\circ}\text{C}$ ), and SF the warmest ( $\sim 18$ – $13$   $^{\circ}\text{C}$ ). The temperature increase in spring (May–Jul) is more dramatic than the fall decrease (Fig. 2) with the NEP still representing the coldest subregion ( $\sim 6$ – $14$   $^{\circ}\text{C}$ ) and SF the warmest ( $\sim 7$ – $18$   $^{\circ}\text{C}$ ). The mean pycnocline depth in September is  $23$  m in both the NEP and GSC and  $32$  m in the SF, but erosion of the mixed layer over the fall leads to all of GB being *well-mixed* by November (Fig. 3). In spring, the opposite trends are observed. GB is *well-mixed* in May, but stratification increases with seasonal warming, such that mean pycnocline depths in July are  $\sim 10$ – $20$  m, with NEP and GSC exhibiting deeper pycnoclines than SF (Fig. 3).

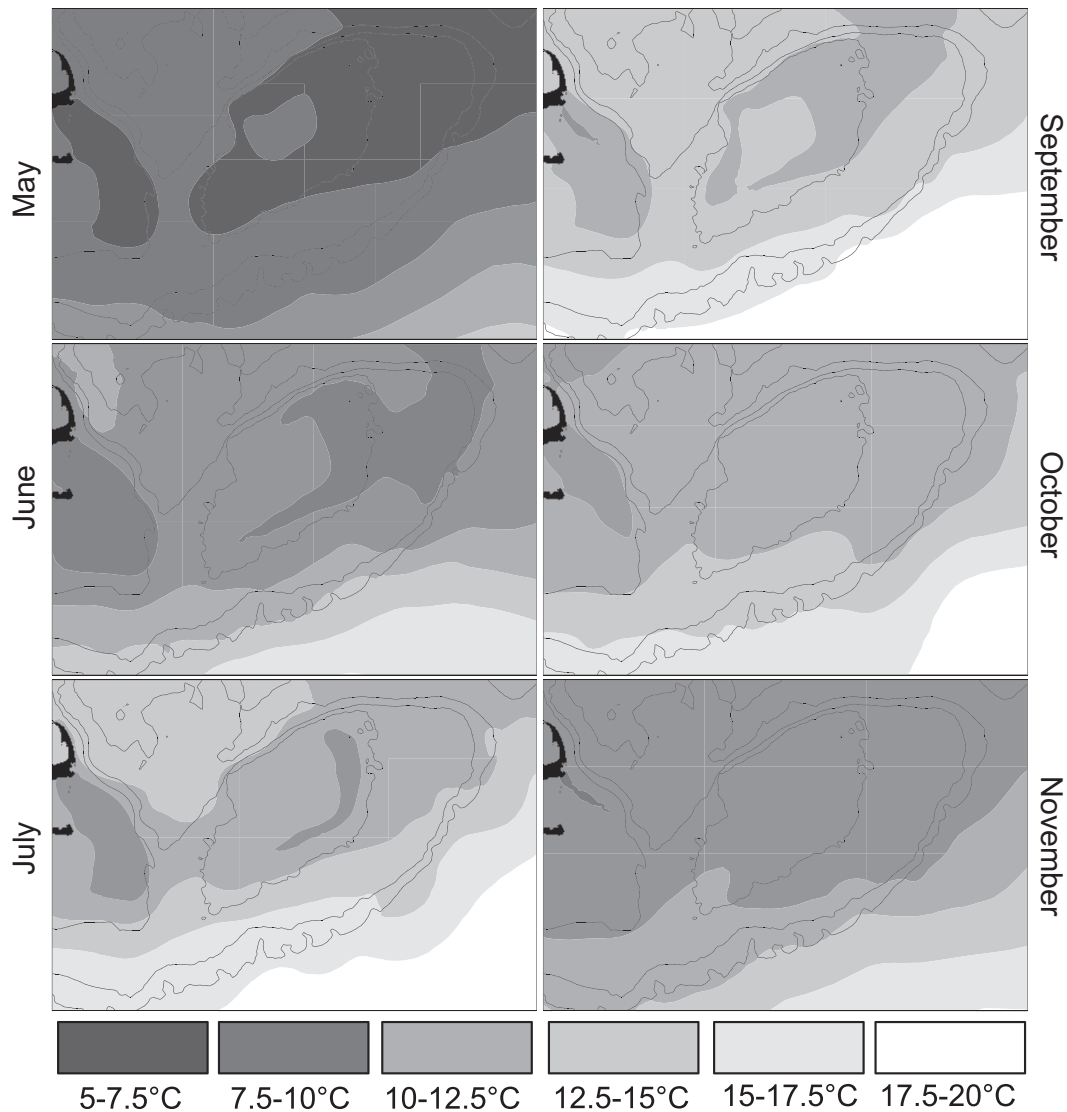


Fig. 2. Sea surface temperature for the middle of (a) May, (b) June, (c) July, (d) September, (e) October and (f) November on GB.

### 2.3. Characterizing beds and connectivity

The geographic extents of the GB subpopulations were delineated by analysis of scallop fishery tow data (Hart and Chute, 2004). Contours of non-negligible scallop density (i.e. >25 scallops per tow) were computed, identifying two distinct continuous regions: one in the Great South Channel (GSC, Fig. 1), and one on eastern GB. The large eastern region was subdivided into two sub-regions: the Northeast Peak and the Southern Flank (NEP, SF, Fig. 1). This distinction was made in order to separate the Canadian and US economic zones along the International Court of Justice (ICJ) line, and to be consistent with previous delineations of these subpopulations (Tremblay et al., 1994).

Simulations initialized 64 particles at every spawn location on a square grid with 4 km spacing within each subpopulation, in order to provide sufficiently high sampling of the spatial variation in the horizontal circulation as well as the vertical shear experienced due to the simulated random walk. This approach resulted in each simulation tracking 30,000–40,000 particles “spawned” within each subpopulation. Initial particle depths were chosen to correspond to the local pycnocline in stratified regions and the mean pycnocline depth in well-mixed regions.

Particle exchange was summarized by defining a “connection fraction”,  $c_{(ij)}$ , which equals the fraction of particles “spawned” in subpopulation  $j$  (where  $j$  is GSC, NEP, or SF) that settled in region  $i$ , where  $i$  can be one of the three subpopulations as well as “downstream” (DS), or “unsuitable habitat” (UH). The DS region was defined as all locations west of 71°W and represents potential supply to scallop populations southwest of GB. UH was defined as any region outside of the subpopulations and upstream (east) of DS, which correspond to locations where no significant scallop densities are observed (Hart and Chute, 2004) and where the suitability of benthic substrate is low (Tian et al., 2009a). Connection fractions were summarized in a  $5 \times 3$  “dispersal matrix” (Botsford et al., 2009).

$$C = \begin{bmatrix} c_{(GSC,GSC)} & c_{(GSC,NEP)} & c_{(GSC,SF)} \\ c_{(NEP,GSC)} & c_{(NEP,NEP)} & c_{(NEP,SF)} \\ c_{(SF,GSC)} & c_{(SF,NEP)} & c_{(SF,SF)} \\ c_{(UH,GSC)} & c_{(UH,NEP)} & c_{(UH,SF)} \\ c_{(DS,GSC)} & c_{(DS,NEP)} & c_{(DS,SF)} \end{bmatrix} \quad (5)$$

where each column corresponds to a particular spawning subpopulation, and each row corresponds to a particular settlement region.



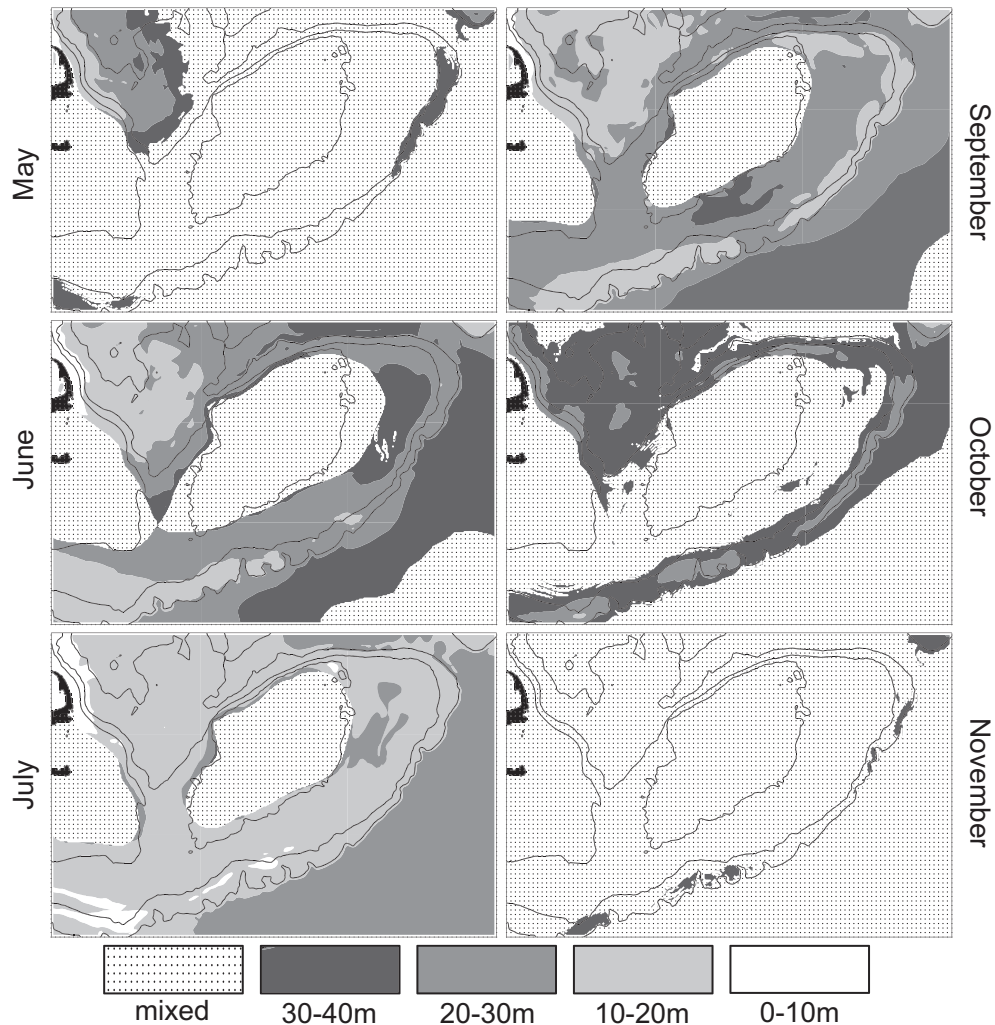


**Fig. 3.** Estimated pycnocline depths for the middle of (a) May, (b) June, (c) July, (d) September, (e) October and (f) November. Dotted regions indicate a well-mixed water column (see text).

Because these five regions are non-overlapping and comprise the entire model domain, the columns of the resulting dispersal matrix each sum to 100%.

### 3. Results

#### 3.1. Depth-distribution and particle transport in fall

Simulated transport of larvae with PLD of 35 days (i.e. assuming  $T_{ind} = 13.5$  °C for all individuals) and passive swimming behavior supported findings from previous studies that used similar assumptions, which all indicate significant drift among the three subpopulations (Fig. 4a–c; Table 1; Tremblay et al., 1994; Tian et al., 2009a). Thirty-nine percent of particles spawned in the GSC were advected DS, and 24% settled in UH, leaving 37% remaining within the metapopulation. GSC-spawned particles were locally retained at approximately the same rate they settled in the combination of the other two subpopulations (20% vs. 17%). In contrast, virtually no NEP-spawned particles left GB or were locally retained (Fig. 4b), and instead the majority settled in UH (61%, Table 1, Fig. 4b). The proportion of NEP-spawned particles retained within the metapopulation was 39% – effectively the same as the GSC – and they settled in both the SF (22%) and GSC (13%).

Thirty-seven percent of particles spawned in the SF settled in UH, and another 14% were lost to DS. Like those from the NEP, local retention of SF-spawned particles was negligible; instead, most were transported to the GSC (45%, Table 1, Fig. 4c).

In the preceding simulation, particles were initialized at the local pycnocline in September, so as to be consistent with observations and previous model investigations (Tremblay and Sinclair, 1990; Tremblay et al., 1994; Tian et al., 2009a). However, particle depth-distribution quickly de-correlated with the pycnocline (Fig. 5). This de-correlation was due in part to large random-walk excursions ( $\Delta z > 20$  m per tidal period) resulting from high mixing, and in part to the seasonal deepening of the pycnocline as the simulation progressed. By the end of the simulation, more than a third of the particles were more than 20 m from the pycnocline. Thus, the depth-distribution resulting from passive behavior is inconsistent with observations. Our results indicate that in order to remain in the pycnocline, larvae would need to overcome net advective and dispersive displacements of  $\sim 20$  m over a tidal cycle, which corresponds to mean swimming speeds of  $\sim 0.4$  mm/s. This is within the range of capabilities reported in the literature (Chia et al., 1984; Tremblay et al., 1994).

To assess how a more realistic larval depth-distribution influences larval drift, we modelled the transport of pycnocline-seeking particles. Results for simulations using  $PLD_{ind} = 35$  d are shown in

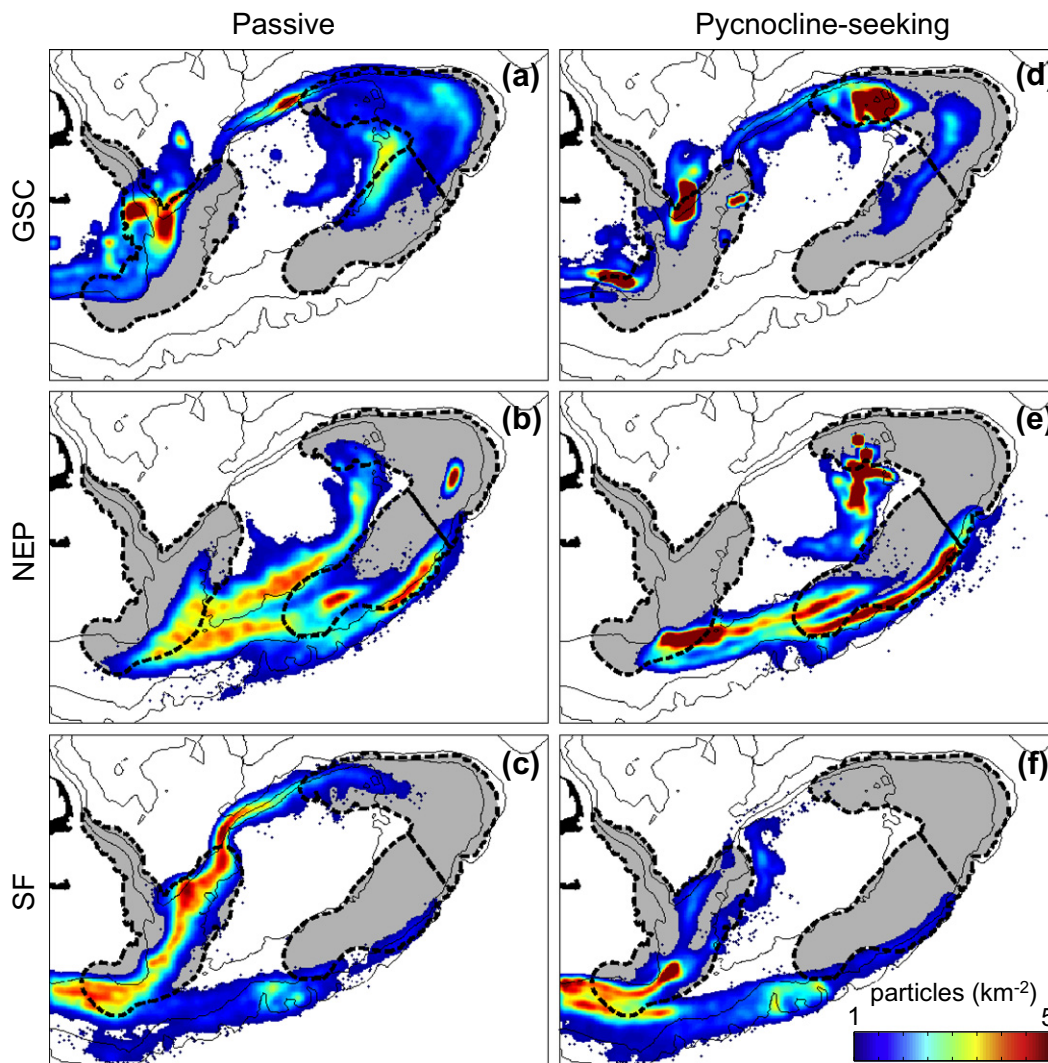


**Fig. 4.** Simulated settlement distribution at the end of the fall simulation for the *passive* (a–c) and *pycnocline-seeking* (d–f) model runs, with PLD = 35 days. The distributions for the GSC-spawned (a and d), NEP-spawned (b and e), and SF-spawned (c and f) particles are each shown separately.

**Table 1**

Dispersal matrices summarizing model simulation results for six different scenarios. *Passive* (top row) and *pycnocline-seeking* (bottom row) behaviors are compared for the fall, with an assumed constant PLD (left column), fall with individually varying PLD (middle column), and spring, with individually varying PLD (right column).

Settle	Spawn								
	Fall, 35 d			Fall, PLD(T)			Spring, PLD(T)		
	GSC	NEP	SF	GSC	NEP	SF	GSC	NEP	SF
<i>Passive</i>									
GSC	20	13	45	18	15	47	4	23	24
NEP	12	4	3	13	4	4	8	4	4
SF	5	22	1	8	16	1	7	9	0
UH	24	61	37	21	65	36	22	63	23
DS	39	0	14	40	0	12	59	1	49
<i>Pycnocline</i>									
GSC	21	12	22	21	13	25	18	0	7
NEP	25	8	0	24	7	0	13	14	1
SF	1	28	1	2	23	1	1	5	0
UH	18	52	14	18	57	43	17	81	51
DS	35	0	63	35	0	31	51	0	41

**Fig. 4d–f and Table 1.** Overall retention within the metapopulation was similar for *pycnocline-seeking* and *passive* behaviors, but there were some pronounced changes in settlement distributions and

the exchange among subpopulations. Connection fractions for GSC-spawned *pycnocline-seeking* particles were not substantially different from the *passive* case, with the notable exception of settlement in the NEP, which doubled (25% vs. 12%) due to the dense aggregation of particles settling inside of the 60 m isobath (Fig. 4d). While settlement distributions for NEP-spawned *pycnocline-seeking* particles were more densely aggregated (Fig. 4e vs. b), connection fractions were essentially unchanged from the *passive* case. Loss of SF-spawned *pycnocline-seeking* particles to DS increased dramatically relative to the *passive* case (63% vs. 14%), due to most particles now being transported in the along-shelf currents. This altered the settlement distribution of SF-spawned *pycnocline-seeking* particles (Fig. 4c vs. f), and reduced the fraction settling in the GSC (22% vs. 45%) and in UH (14% vs. 37%).

### 3.2. Effect of temperature-dependent PLD

To assess the extent to which temperature variability influences dispersal, we simulated larval transport using  $PLD_{ind}$  based on each individual's thermal history. Variation in the fall temperature fields led to a range of  $PLD_{ind}$  that was similar to previous estimates (i.e. Fig. 6 vs. 30–40 d; Tremblay et al., 1994). This range was larger for

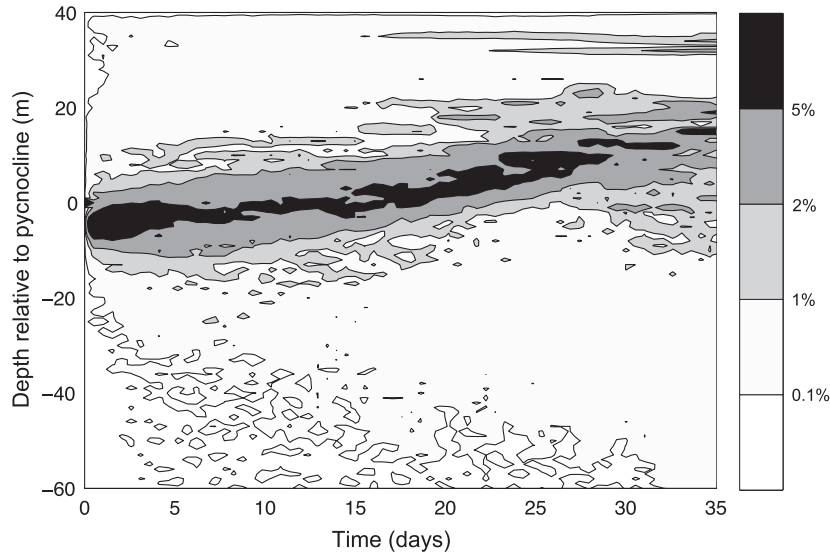


**Fig. 5.** Time-series of particle depth-distribution relative to the local pycnocline in stratified regions (% of total particles per meter depth) for the *passive* simulation in fall.

*passive* than for *pycnocline-seeking* particles (30–54 d *passive* vs. 27–43 d), due to their broader distribution across vertical temperature gradients. The mean fall  $PLD_{ind}$  was 37 d for *passive* and 36 d for *pycnocline-seeking* behaviors, indicating that the average temperature along the particle paths was slightly lower than 13.5 °C for which  $PLD = 35$  d. The longer  $PLD$  associated with the *passive* simulation was due to a greater proportion of particles being distributed in the colder waters below the thermocline.

While the difference in mean  $PLD$  of one day due to depth-distribution in the fall was statistically significant ( $p < 0.001$ ), it was trivial compared to the difference in mean  $PLD$  between fall and spring. The mean temperature near the pycnocline in spring is  $\sim 9.5$  °C, which corresponds to a mean  $PLD$  of 48 days – almost two weeks longer than the mean  $PLD$  in fall. Spring simulations

using  $PLD_{ind}$  based on the individual's thermal history also resulted in a wide range of  $PLD_{ind}$  (40–60 d *passive* vs. 39–53 d *pycnocline-seeking*). The mean spring  $PLD_{ind}$  was 49 days for *passive* and 47 days for *pycnocline-seeking* particles, indicating the average temperature along their paths was  $\sim 9.5$  °C. The two-day difference in  $PLD$  is statistically significant ( $p < 0.001$ ), but again, trivial compared to the inter-seasonal variability.

There were no substantial differences in predicted dispersal or connectivity for fall simulations in which  $PLD_{ind} = 35$  d was compared with those for which  $PLD_{ind}$  was based on thermal history (Fig. 7 vs. Fig. 4; Table 1). The only exception was for *pycnocline-seeking* particles spawned in the SF, for which individually varying  $PLD$  reduced the fraction lost to DS (63% vs. 31%) and increased the fraction settling in UH (14% vs. 43%). These changes were due to

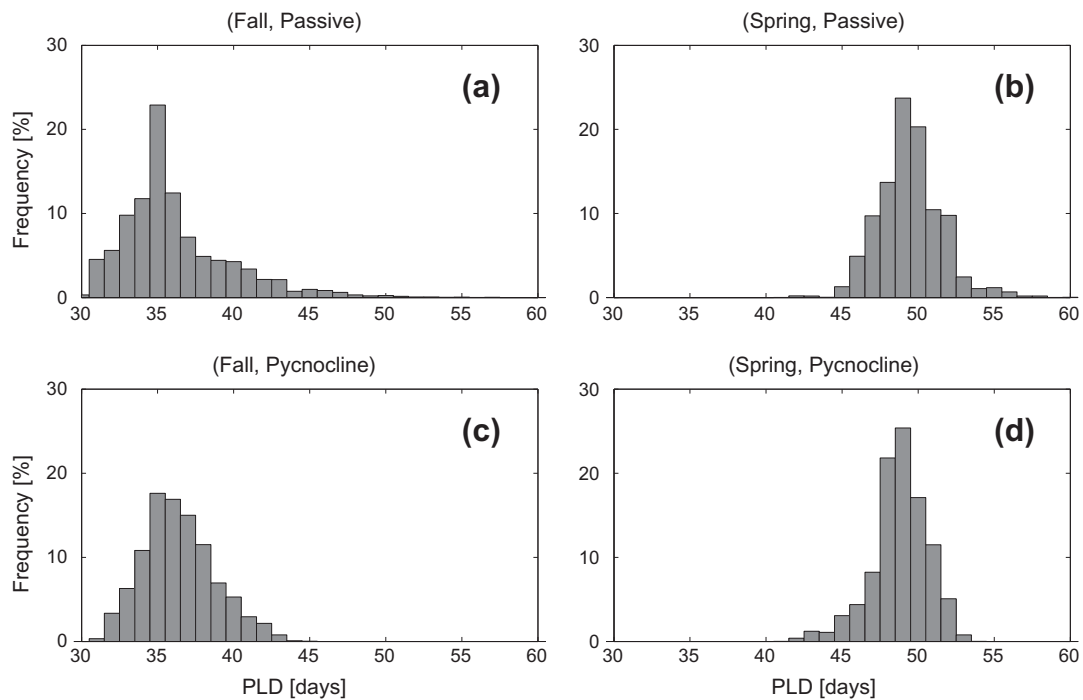


**Fig. 6.** Histogram of  $PLD$  for (a) fall, *passive*; (b) fall, *pycnocline-seeking*; (c) spring, *passive*; and (d) spring, *pycnocline-seeking* simulations with individually varying  $PLD$ .



accelerated growth in the warm southern flank slope waters and resulted in more particles reaching settlement size before they could be advected out of the domain. Spring simulations exhibited the same lack of sensitivity as seen in fall, such that results for temperature-dependent  $PLD_{ind}$  (Fig. 8) were effectively the same as those for  $PLD = 48$  d (not shown). Hence, all results discussed below are for the temperature-dependent case.

### 3.3. Particle transport in spring vs. fall

Settlement distributions for larvae with  $PLD_{ind}$  based on individual thermal history and *passive* behavior were similar in both the spring and fall (Fig. 8a–c vs. Fig. 7a–c), indicating that longer spring PLDs coincidentally balanced slower spring currents. However, there were several noteworthy differences in exchange among the subpopulations (Table 1). For GSC-spawned particles, local retention was reduced relative to fall (4% vs. 18%), which corresponded with an increased loss to DS (59% vs. 40%). Settlement in the GSC increased for NEP-spawned particles (23% vs. 15%), but decreased for those spawned in the SF (24% vs. 47%). Loss of SF-spawned particles to DS also increased (49% vs. 12%). These differences can be explained in terms of seasonal changes in the strength of the around-bank gyre (Naimie et al., 1994, 2001). This recirculatory flow was weak early in the spring, causing particles

from the GSC and SF to experience low retention and high losses. Strengthening of the gyre with increased stratification later in the spring caused particles from the NEP to have higher retention. The reverse effect occurs in fall (i.e. the gyre is strong early in the season but weak later) causing higher retention of GSC- and SF-spawned particles and lower retention of NEP-spawned particles.

Altering depth-distribution in the spring had a pronounced effect on both settlement distributions and associated connection fractions (Fig. 8d–f vs. Fig. 8a–c, Table 1). In spring, *pycnocline-seeking* behavior increased local retention of GSC-spawned particles as compared to the *passive* case (18% vs. 4%, Table 1) and decreased settlement of NEP-spawned particles in the GSC (0% vs. 23%). This is in stark contrast to fall, when depth-distribution had negligible effects on these connection fractions. Additionally, *pycnocline-seeking* particles from the NEP settled more frequently in UH (81% vs. 63%). Particles from SF also experienced less settlement in the GSC (7% vs. 24%), and instead settled in UH (51% vs. 23%). These changes can be explained by the fact that on-bank retention during spring requires plankton be deep in the water column (Werner et al., 1993; Lynch et al., 1998; Gentleman, 2000; Lough and Manning, 2001).

Settlement distributions for *pycnocline-seeking* particles in the spring were similar to those having the same behavior in fall (Fig. 8d–f vs. Fig. 7d–f). However, this similarity was not borne

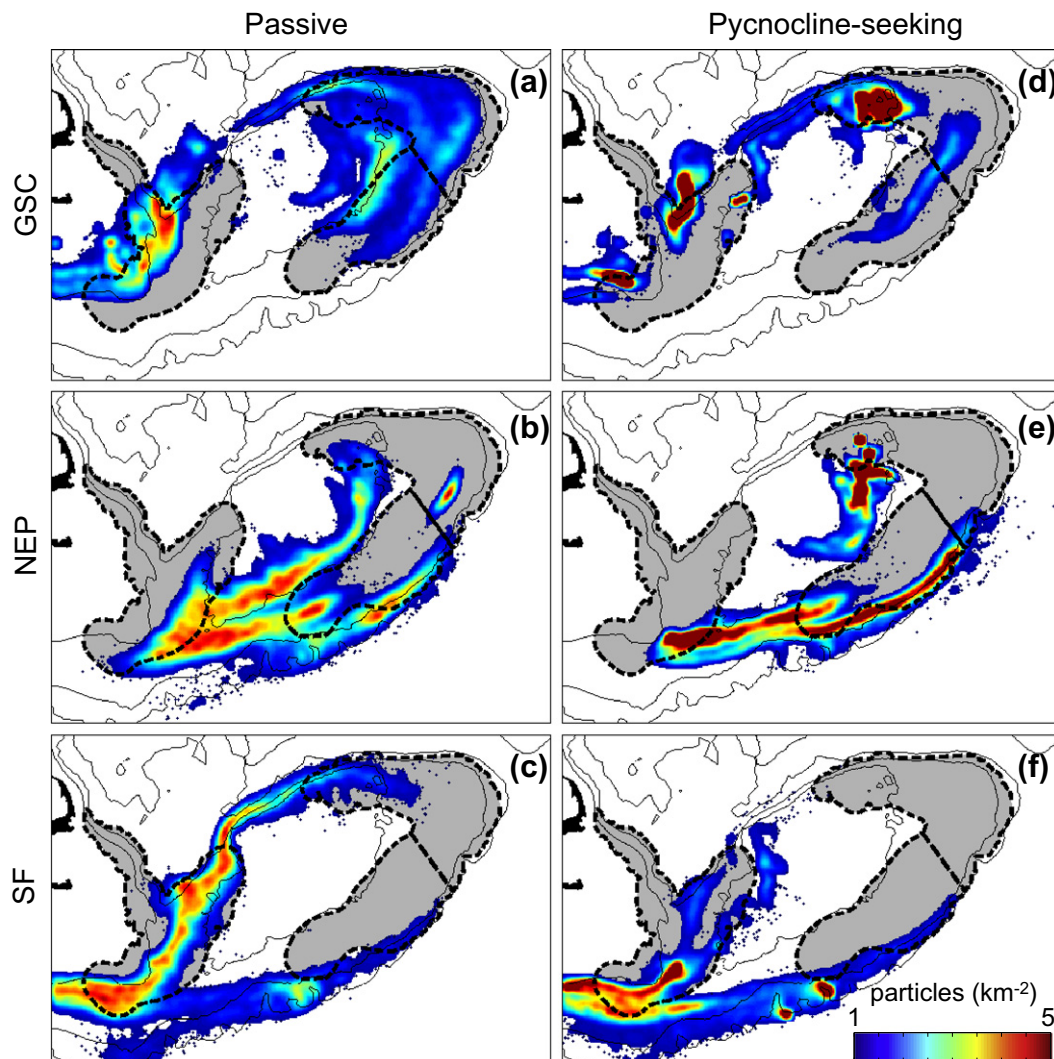
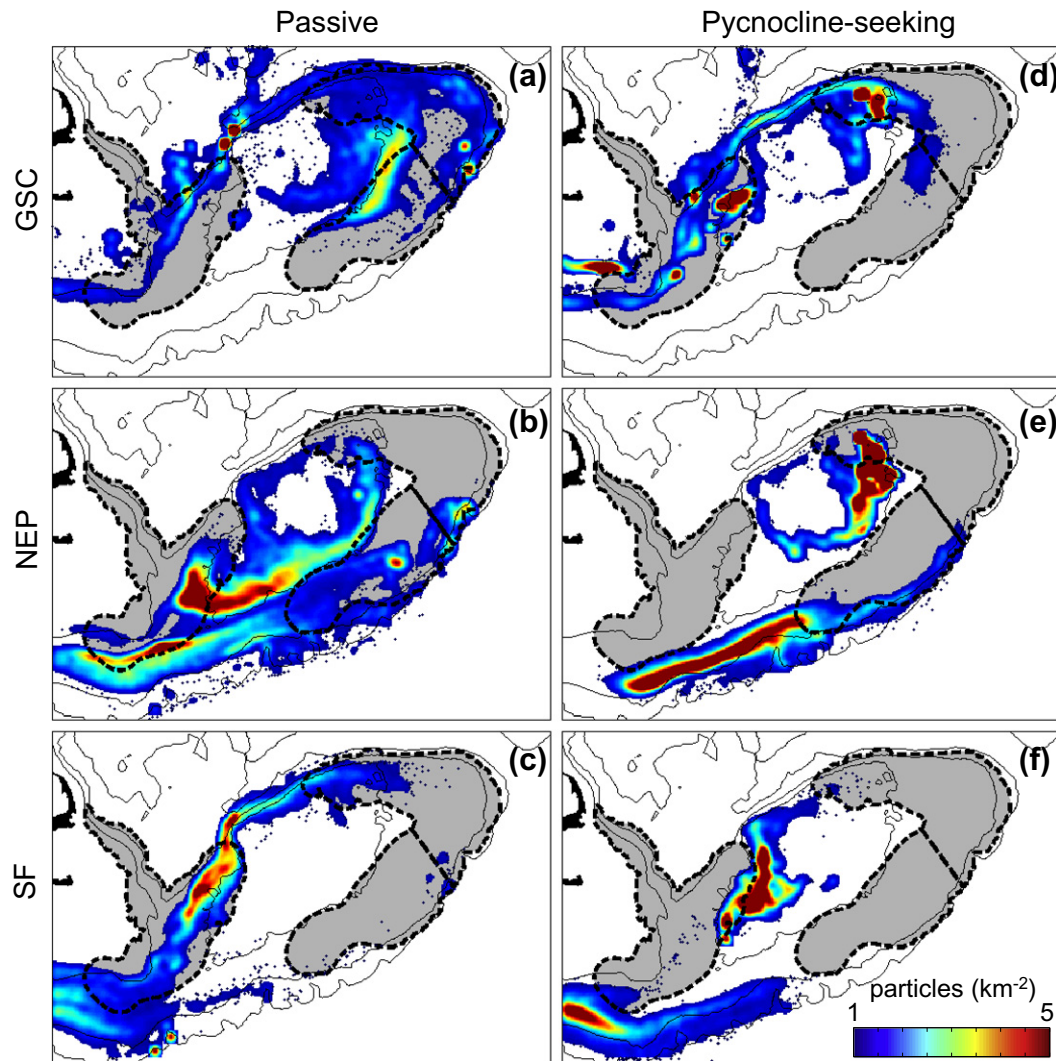


Fig. 7. Simulated settlement distribution at the end of the fall simulation for the *passive* (a–c) and *pycnocline-seeking* (d–f) model runs, with individually varying temperature-dependent PLD. The distribution for the GSC-spawned (a and d), NEP-spawned (b and e), and SF-spawned (c and f) particles are each shown separately.





**Fig. 8.** Simulated settlement distribution at the end of the spring simulation for each subpopulation after the *passive* (a–c) and *pycnocline-seeking* (d–f) model runs with individually varying temperature-dependent PLD. The distribution for the GSC-spawned (a and d), NEP-spawned (b and e), and SF-spawned (c and f) particles are each shown separately.

out in the connection fractions due to inter-seasonal differences in environmental conditions. Loss of GSC-spawned *pycnocline-seeking* particles to DS was greater in the spring than in fall (51% vs. 35%). The fraction of NEP-spawned particles settling in the GSC decreased (0% vs. 13%), whereas both local retention and settlement in UH increased (14% vs. 7% and 81% vs. 57%). Similarly, SF-spawned particles were less likely to settle in GSC (7% vs. 25%), but more likely to be transported DS or settle in UH (and 41% vs. 31% and 51% vs. 43%). These differences arose due to the aggregation of larvae at the shallow pycnocline, which causes them to be transported off GB by the strong along-shelf flow.

## 4. Discussion

### 4.1. Depth-distribution in fall

Our results for dispersal of *passive* larvae in the fall are consistent with previous model studies (Tremblay et al., 1994; Tian et al., 2009a), showing the GSC-spawned larvae can be locally retained or settle in both the NEP and SF, whereas local retention of NEP and SF subpopulations is negligible and larvae from both regions settle in the GSC (Fig. 9). This indicates that our simplifying

assumptions about ascent, descent and residual advection were reasonable and further, our work has highlighted some previously unrecognized features of the metapopulation dynamics. For example, while the GSC is the most locally retentive in fall, overall rates of retention within the metapopulation in fall are roughly equal for each of the three subpopulations. Additionally, there are noteworthy differences among the subpopulations with regard to which can supply larvae to DS populations, as well as the relative proportion predicted to settle in UH (Fig. 9, Table 1). Thus, our results demonstrate that the sources, retention and losses are unique for each subregion, but their tight coupling through advective exchange of larvae indicates that the function of each subpopulation needs to be considered to study the dynamics of the metapopulation of *P. magellanicus* on GB.

Previous studies were able to identify certain simulated behaviors as unrealistic because they resulted in horizontal distributions that were inconsistent with observations (e.g. “fixed-depth”, Tremblay et al., 1994). By the same approach, we have demonstrated that simulations of passive behavior result in unrealistic vertical distributions (Fig. 5), suggesting that model estimates of larval dispersal based on passive behavior may be biased. Our novel simulation of *pycnocline-seeking* particles was designed to reflect observed depth-distributions. In contrast to the *passive*

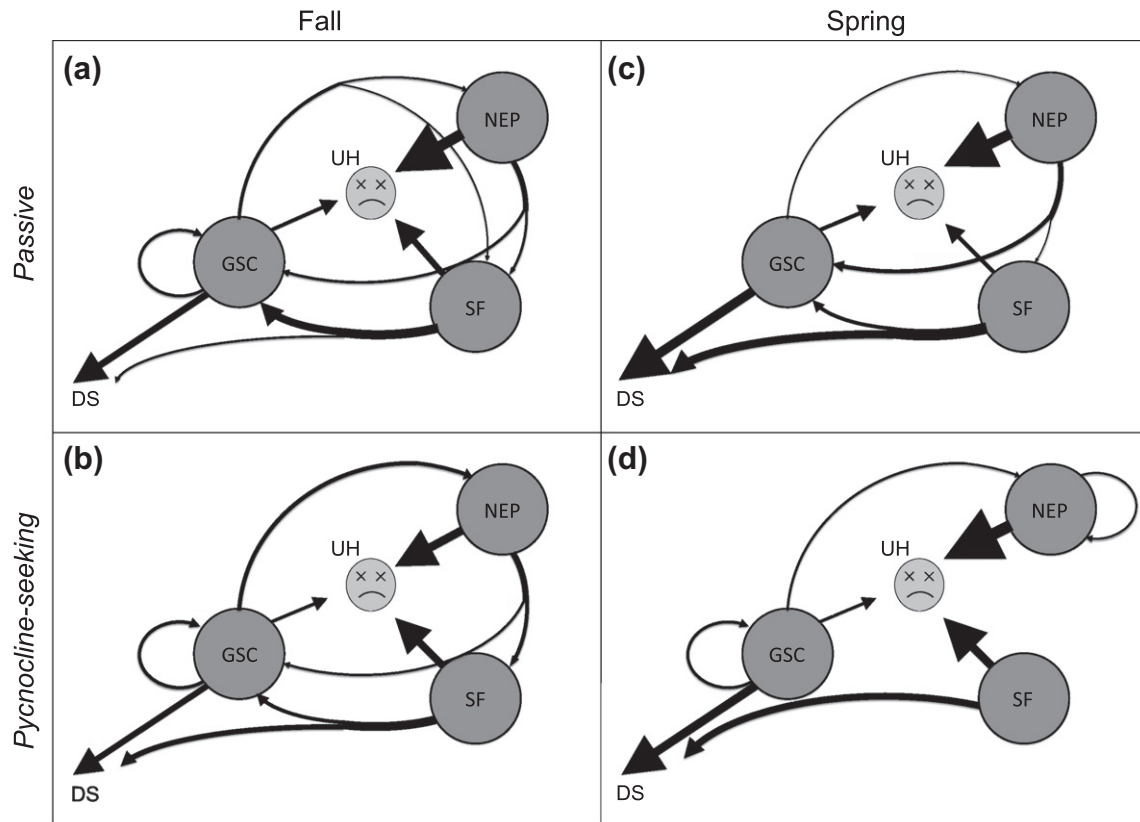


**Fig. 9.** Schematic diagrams of model-estimated connectivity for the (a) fall, *passive*; (b) fall, *pycnocline-seeking*; (c) spring, *passive*; and (d) spring, *pycnocline-seeking* cases. Each arrow illustrates the transport of particles among the geographic regions (GSC, NEP, SF, DS and UH), with the thickness of the arrow proportional to the corresponding connection fraction. Small connection fractions (<8%) have been omitted from the graphs.

simulation, *pycnocline-seeking* behavior aggregated GSC-spawned particles on the NEP, where high densities of late-stage larvae and adult scallops are observed (Fig. 4e; Tremblay and Sinclair, 1992; Hart and Chute, 2004). Hence, *pycnocline-seeking* behavior seemed to improve modelled distributions on the NEP, but whether this is the case for other regions is difficult to determine without more data for horizontal distributions of late-stage larvae.

The effect of larval depth-distribution on predicted settlement was different for each subpopulation, such that there is a complex relationship between depth-distribution and GB metapopulation dynamics. Changing from *passive* to *pycnocline-seeking* behavior strengthened connectivity from the GSC to NEP, had little effect on NEP-spawned particles, and caused SF-spawned particles to be advected DS instead of being retained in the GSC (Fig. 4, Fig. 9, Table 1). These effects corresponded to changes in the associated connection fractions by factors of 2–5 (Table 1), comparable to the estimated effects of variability in the circulation (Tian et al., 2009a). This is far greater an effect of depth-distribution than previous estimates based on other simplified behaviors (e.g. fixed-depths, surface-seeking, etc.; Tremblay et al., 1994; Tian et al., 2009a).

The influence of behavior may be different than our results indicate, as larval behaviors are more complex than characterized by our model. Our *pycnocline-seeking* behavior is idealized. For example, it neglects any high-frequency interactions of the physics and biology. As well, laboratory studies show that larger veliger larvae may swim below the pycnocline (Gallager et al., 1996), which could have significant effects on the retention of NEP- and SF-spawned larvae, as the strength of the around-bank gyre increases with depth. Furthermore, aggregation at the pycnocline has not been linked to any particular behavioral mechanism, and it is

possible that larvae are responding to changes in environmental variables that are correlated with the pycnocline (e.g. temperature, food etc.), as opposed to responding to density *per se*. As well, *P. magellanicus* may vertically migrate to decrease the risk of predation as well as increase probability of retention (Manuel et al., 1996). This suggests the need for more lab, field and model studies focused on understanding how the observed depth-distribution emerges from the complex interactions of larvae with their environment.

#### 4.2. Planktonic larval duration

Previous model studies assumed that PLD was the same for all scallop larvae on GB, and that the mean PLD in the fall was ~35 days based on mean temperatures (Tremblay et al., 1994; Tian et al., 2009a). To investigate the effect of individual thermal history, we developed a model for temperature-dependent PLD, using a  $Q_{10}$  relationship. Our simple model estimates that the 4 °C cooler mean temperature in spring extends the mean PLD by about 2 weeks. Intra-seasonal regional variations in temperatures (Fig. 2) led to individual PLDs ranging by more than 10 days (Fig. 6). Changing between *passive* vs. *pycnocline-seeking* behaviors led to statistically significant variations in mean PLD of 1–2 days (Fig. 6), with *passive* being systematically longer, due to particles below the thermocline experiencing colder temperatures. PLD temperature-dependence needs to be considered when larvae experience different temperatures over prolonged periods of time (e.g. variations between years, seasons, regions and/or depths).

Simulations with PLD based on thermal history had similar settlement distributions and connection fractions to those for which PLD was set at a constant mean value (Fig. 6, Table 1), which sup-

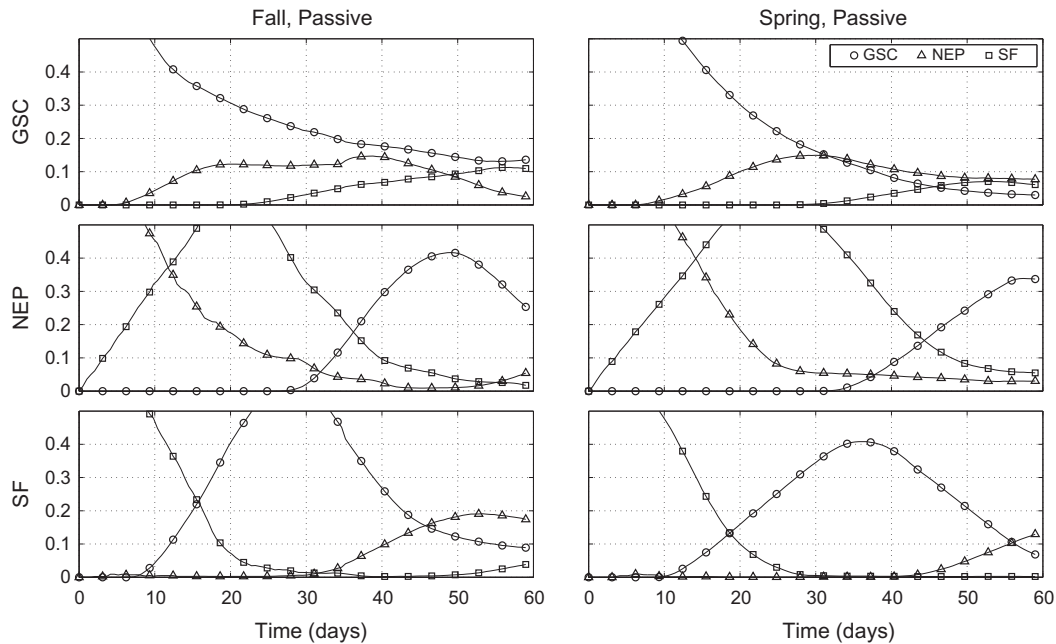


**Fig. 10.** Connection-fractions plotted as a function of PLD for the *passive* simulation in fall (left column) and spring (right column). Connection fraction from the source (labeled on the y-axis) to GSC is labeled with circles, while the connection fraction from source to NEP is marked with triangles and source to SF is marked with squares.

ports previous studies of larval transport in fall (Tremblay et al., 1994; Tian et al., 2009a). The one notable exception was for SF-spawned *pycnocline-seeking* particles, which showed a dramatic reduction in DS losses due to the influence of the warm slope water. Supply of GB larvae to scallop populations along the New-England Shelf and Mid-Atlantic Bight may therefore be sensitive to processes causing pronounced temperature variations on the SF (e.g. intrusion of warm-core rings).

While our results show that variation in mean PLD of 1–2 days had little effect, change in mean PLD of a few days does affect retention and exchange among the subpopulations in both seasons. A difference of 5 days in the seasonal mean PLD changes predicted connection fractions by factors of 2–10 for certain subpopulations (Fig. 10). This difference in mean PLD is well within confidence intervals, as variation in settlement size leads to a range in PLD of 10 days in the fall (Tremblay et al., 1994) and changing  $Q_{10}$  from 2 to 2.5 extends the estimated mean spring PLD by 5 days. Furthermore, larvae may extend their PLD if the local benthic habitat is not a suitable substrate (Culliney, 1974; Tremblay et al., 1994), and such behavior has been shown to significantly affect larval transport for other species (Savina et al., 2010). This could be significant for the *P. magellanicus* metapopulation, given that our results – which did not simulate such behavior – predict large losses due to settlement in UH (Fig. 9 and 14–81%, Table 1). This indicates the need to improve our understanding of factors introducing variation in the PLD.

#### 4.3. Spawning seasonality

We found that overall retention within the GB metapopulation was lower in spring than in fall. As previously hypothesized, this was due to reduced recirculation of larvae in the around-bank gyre prior to stratification. The associated losses of SF and GSC-spawned particles to DS suggest that larvae from these two subpopulations are prime candidates for supplying scallop populations along the New-England Shelf and Mid-Atlantic Bight. However, retention of NEP-spawned particles was higher in spring than in fall, due to intensification of the around-bank gyre in late spring, as compared

to the erosion of the gyre in late fall. This suggests high sensitivity of larval connectivity to climate-related changes in stratification.

We showed that depth-distribution influences dispersal of *P. magellanicus* larvae, as has been shown for other planktonic species in the region (Werner et al., 1993; Lough and Manning, 2001). In fact, changing between *passive* and *pycnocline-seeking* behavior had a larger impact on connectivity in spring than in fall (Fig. 10, Table 1). The *pycnocline-seeking* behavior was based on observations made in the fall, but hydrographic conditions in spring are different from those in the fall (Fig. 2), such that associated larval behaviors may also be different. Our ability to confidently quantify retention and exchange in spring is currently limited by lack of observations.

In addition to transport-related connectivity, the number of larvae ultimately recruiting to the metapopulation will depend on survivorship in each spawning season. Survivorship in the spring would be reduced relative to that in fall due to the increased PLD, if mortality rates were the same between seasons. However, spring mortality rates are likely lower than in fall, because larval mortality rates are typically reduced for lower temperatures (Houde, 1989). For example, if the  $Q_{10}$  for mortality is the same as that assumed for PLD, then these effects would cancel out and survivorship in both seasons would be comparable. This warrants more study, along with other factors influencing recruitment, including fecundity and post-settlement survival. In order to understand the metapopulation dynamics for *P. magellanicus* on GB, these additional biological processes must be examined.

#### 5. Summary

Effective management of *P. magellanicus* for any particular sub-region of GB requires a process-oriented understanding of the effect of climate on the dynamics of this metapopulation. Here, we have shown that biological responses to changes in temperature and stratification affect larval transport among GB subpopulations, as well as the extent to which they can supply downstream regions. Specifically, variation in larval depth-distribution, planktonic larval duration, and the previously-overlooked issue of spawning seasonality result in changes to retention and exchange

that are comparable to the effect of interannual variation in the currents. We have also demonstrated that uncertainty associated with these biological factors leads to high uncertainty in predicted larval dispersal. As such, our work has emphasized the need to conduct specific lab, field and modelling studies in order to improve predictions.

## Acknowledgments

The authors are very grateful to D. Hart, S. Smith and I. Jonsen for providing important demographic scallop data and expert guidance, to J. Tremblay, A. Curtis, E. Head and C. Hannah for their discussion and commentary on the design of this study, to D. Levy for support in the data analysis, and to G. Fung, K. Latham and K. Svendsen for their editorial assistance. This work was supported by Fisheries and Oceans Canada, the Gulf of Maine Research Initiative, and the National Science and Engineering Research Council of Canada.

## References

- Beaumont, A.R., Barnes, D.A., 1992. Aspects of veliger larval growth and byssus drifting of the spat of *Pecten maximus* and *Aequipecten* (*Chlamys*) *opercularis*. ICES Journal of Marine Science 49, 417–423.
- Botsford, L.W., White, J.W., Coffroth, M.A., Paris, C.B., Planes, S., Shearer, T.L., Thorrold, S.R., Jones, G.P., 2009. Connectivity and resilience of coral reef metapopulations in marine protected areas: matching empirical efforts to predictive needs. Coral Reefs 28, 327–337.
- Butman, B., Beardsley, R., 1987. The physical oceanography of Georges Bank: Introduction and summary. In: Backus, R.H. (Ed.), Georges Bank. The MIT Press, Cambridge, Mass, pp. 88–98.
- Chen, C., Liu, H., Beardsley, R., 2003. An unstructured grid, finite-volume, three dimensional, primitive equations ocean model: application to coastal ocean and estuaries. Journal of Atmospheric and Oceanic Technology 20, 159–186.
- Chia, F., Buckland-Nicks, J., Young, C., 1984. Locomotion of marine invertebrate larvae – a review. Canadian Journal of Zoology-Revue Canadienne de Zoologie 62, 1205–1222.
- Cowen, R., Sponagule, S., 2009. Larval dispersal and marine population connectivity. Annual Review of Marine Science 1, 443–466.
- Cullinney, J., 1974. Larval Development of the giant scallop *Placopecten magellanicus* (Gmelin). Biological Bulletin 147, 321–332.
- DiBacco, C., Robert, G., Grant, J., 1995. Reproductive cycle of the sea scallop, *Placopecten magellanicus* (Gmelin, 1791), on northeastern Georges Bank. Journal of Shellfish Research 14, 59–69.
- Fiksen, O., Jorgensen, C., Kristiansen, T., Vikebo, F., Huse, G., 2007. Linking behavioural ecology and oceanography: larval behaviour determines growth, mortality and dispersal. Marine Ecology Progress Series 347, 195–205.
- Gallager, S., Manuel, J., Manning, D., O'Dor, R., 1996. Ontogenetic changes in the vertical distribution of giant scallop larvae, *Placopecten magellanicus*, in 9-m deep mesocosms as a function of light, food, and temperature stratification. Marine Biology 124, 679–692.
- Gentleman, W.C., 2000. Factors controlling the seasonal abundance and distribution of *Calanus finmarchicus* in the Gulf of Maine/Georges Bank region. PhD thesis, Dartmouth College, Hanover, NH.
- GLOBEC, 1992. Northwest Atlantic Implementation Plan. Report Number 6, June 1992.
- Hannah, C.G., Naimie, C.E., Loder, J.W., Werner, F.E., 1998. Upper-ocean transport mechanisms from the Gulf of Maine to Georges Bank, with implications for Calanus supply. Continental Shelf Research 17, 1887–1911.
- Hart, D., Chute, A., 2004. Sea scallop, *Placopecten magellanicus*, life history and habitat characteristics. Woods Hole, MA, National Marine Fisheries Service.
- Hill, A.E., 1991. A mechanism for horizontal zooplankton transport by vertical migration in tidal currents. Marine Biology 111, 485–492.
- Houde, E.D., 1989. Comparative growth, mortality and energetics of marine fish larvae. Fishery Bulletin, US 87, 471–495.
- Johnson, C., Pringle, J., Chen, C., 2006. Transport and retention of dormant copepods in the Gulf of Maine. Deep Sea Research Part II 53, 2520–2536.
- Lough, G.R., Manning, J.P., 2001. Tidal-front entrainment and retention of fish larvae on the southern flank of Georges Bank. Deep Sea Research Part II – Topical Studies in Oceanography 48, 631–644.
- Lynch, D.R., Gentleman, W.C., McGillicuddy, D., Davis, C.S., 1998. Biological/physical simulations of *Calanus finmarchicus* population dynamics in the Gulf of Maine. Marine Ecology Progress Series 169, 189–210.
- Manuel, J., Gallager, S., Pearce, C., Manning, D., O'Dor, O., 1996. Veligers from different populations of sea scallop *Placopecten magellanicus* have different vertical migration patterns. Marine Ecology Progress Series 142, 147–163.
- Metaxas, A., Saunders, M., 2009. Quantifying the “bio-” components in biophysical models of larval transport in marine benthic invertebrates: advances and pitfalls. Biological Bulletin 216, 257–272.
- Miller, C.B., Lynch, D.R., Carlotti, F., Gentleman, W.C., Lewis, C.V.W., 1998. Coupling of an individual-based population dynamic model of *Calanus finmarchicus* to a circulation model for the Georges Bank region. Fisheries Oceanography 7, 219–234.
- Naidu, S., Robert, G., 2006. Fisheries sea scallop, *Placopecten magellanicus*. In: Shumway, S.E., Parsons, G.J. (Eds.), Scallops: Biology, Ecology and Aquaculture, second ed. Elsevier, Amsterdam, pp. 869–905.
- Naimie, C.E., Loder, J.W., Lynch, D.R., 1994. Seasonal variation of the three-dimensional residual circulation on Georges Bank. Journal of Geophysical Research 99 (C8), 15967–15989.
- Naimie, C., Limeburner, R., Hannah, C., Beardsley, R., 2001. On the geographic and seasonal patterns of the near-surface circulation on Georges Bank – from real and simulated drifters. Deep-Sea Research part II – Topical Studies in Oceanography 48, 501–518.
- Neuheimer, A., Taggart, C., 2007. The growing degree-day and fish size-at-age: the overlooked metric. Canadian Journal of Fisheries and Aquatic Sciences 64, 375–385.
- Pringle, J., 2006. Sources of variability in Gulf of Maine circulation, and the observations needed to model it. Deep-Sea Research Part II – Topical Studies in Oceanography 53, 2457–2476.
- Savina, M., Lacroix, G., Ruddick, K., 2010. Modelling the transport of common sole larvae in the southern North Sea: influence of hydrodynamics and larval vertical movements. Journal of Marine Systems 81, 86–98.
- Shanks, A., 2009. Pelagic Larval duration and dispersal distance revisited. Biological Bulletin 216, 373–385.
- Thomson, R.E., Fine, I.V., 2003. Estimating mixed layer depth from oceanic profile data. Journal of Atmospheric and Oceanic Technology 20, 319–329.
- Tian, R., Chen, C., Stokesbury, K., Rothschild, B., Cowles, G., Xu, Q., Hu, S., Harris, B., Marino, M., 2009a. Modeling the connectivity between sea scallop populations in the Middle Atlantic Bight and over Georges Bank. Marine Ecology Progress Series 380, 147–160.
- Tian, R., Chen, C., Stokesbury, K., Rothschild, B., Xu, Q., Hu, S., Cowles, G., Harris, B., Marino, M., 2009b. Sensitivity analysis of sea scallop (*Placopecten magellanicus*) larvae trajectories to hydrodynamic model configuration on Georges Bank and adjacent coastal regions. Fisheries Oceanography 18, 173–184.
- Tremblay, M., Sinclair, M., 1990. Sea scallop larvae *Placopecten magellanicus* on Georges Bank – vertical distribution in relation to water column stratification and food. Marine Ecology Progress Series 61, 1–15.
- Tremblay, M., Sinclair, M., 1992. Planktonic sea scallop larvae (*Placopecten magellanicus*) in the Georges Bank region: broadscale distribution in relation to physical oceanography. Canadian Journal of Fisheries and Aquatic Sciences 49, 1597–1615.
- Tremblay, M., Loder, J., Werner, F., Naimie, C., Page, F., Sinclair, M., 1994. Drift of sea scallop larvae *Placopecten magellanicus* on Georges Bank – a model study of the roles of mean advection, larval behavior and larval origin. Deep-Sea Research Part II – Topical Studies in Oceanography 41, 7–49.
- Visser, A.W., 1997. Using random walk models to simulate the vertical distribution of particles in a turbulent water column. Marine Ecology Progress Series 158, 275–281.
- Werner, F., Page, F., Lynch, D., Loder, J., Lough, R., Perry, R., Greenberg, D., Sinclair, M., 1993. Influences of mean advection and simple behavior on the distribution of cod and haddock early life stages on Georges Bank. Fisheries Oceanography 2, 43–64.
- Zimmerman, J.T.F., 1979. On the Euler–Lagrange transformation and the Stokes' drift in the presence of oscillatory and residual currents. Deep Sea Research Part A 26, 505–520.